Lyapunov-Based Adaptive State of Charge and State of Health Estimation for Lithium-Ion Batteries

Hicham Chaoui, *Senior Member, IEEE*, Navid Golbon, *Member, IEEE*, Imad Hmouz, Ridha Souissi, and Sofiène Tahar, *Senior Member, IEEE*

***Abstract*—This paper presents an adaptive state of charge (SOC) and state of health (SOH) estimation technique for lithium-ion batteries. The adaptive strategy estimates online parameters of the battery model using a Lyapunov-based adaptation law. Therefore, the adaptive observer stability is guaranteed by Lyapunov's direct method. Since no *a priori* knowledge of battery parameters is required, accurate estimation is still achieved, although parameters change due to aging or other factors. Unlike other estimation strategies, only battery terminal voltage and current measurements are required. Simulation and experimental results highlight the high SOC and SOH accuracy estimation of the proposed technique.**

***Index Terms*—Adaptive observer, lithium-ion batteries, Lyapunov stability, state of charge (SOC), state of health (SOH).**

I. Introduction

LITHIUM-ION batteries have received an increasing interest from the scientific community. Unlike other types of batteries such as lead acid, nickel cadmium (NiCd), and nickel metal hydride (NiMH), they offer higher energy efficiency and power density [1], [2]. Moreover, several other advantages, such as low steady-state float current, light weight, small size, wide temperature operation range, rapid charge capability, long life cycle, low self-discharge rate, no memory effects, and absence of hydrogen outgassing, make them good candidates for many applications such as laptops, mobile phones, and electric vehicles [3]. However, optimal energy utilization and minimization of degradation effects are among the typical challenges to be faced. State of charge (SOC) and state of health (SOH), which are both expressed in percentage, are the equivalent for batteries of an energy and a lifetime gauge, respectively. Therefore, the accuracy of SOC and SOH algorithms remains an important aspect in battery management systems (BMS) because a bad SOC estimation might significantly damage the battery and ultimately result in reduced battery life.

Conventional SOC estimation techniques are known for their simplicity. The coulomb counting method, which is also called ampere-hour (Ah) balancing method, is a rational way to estimate a battery's SOC [4], [5]. In this technique, the battery's incoming and departing currents are measured and integrated through time to determine SOC. However, startup and current sensor errors are accumulated, which leads to a drift and poor precision, since the process is open-loop based [6]. Moreover, changes to the batteries' capacity as they age are not taken into account. This method has some serious drawbacks [4]. Nevertheless, it remains the simplest approach for real-time industrial applications. On the other hand, open-circuit voltage (OCV) can be used to determine a battery SOC since its voltage is correlated with the electrolyte concentration that varies with the battery charge status [7], [8]. However, this is true only when the battery reaches an equilibrium state (i.e., no current flows through the battery for several minutes or hours). Moreover, this relationship is affected by temperature and aging since capacity is known to gradually decrease with charge and discharge cycles along with depth of discharge. A combination between the aforementioned two methods yields a hybrid estimation technique. Thus, the coulomb counting method is used in operation (i.e., current is flowing into and out of the battery), and whenever the battery reaches an equilibrium state, the SOC is updated with the OCV method to reset accumulated errors. However, some applications require a continuous operation and do not allow batteries to reach an equilibrium state. This raises the urgency of considering other SOC estimation alternatives.

Several robust and accurate estimation techniques are proposed at the cost of higher computational complexity [9], [10]. An accurate SOC estimation technique [11] is proposed using a reduced-order observer. However, it requires the knowledge of the battery's parameters, which results in accuracy reduction as batteries age. This drawback has been overcome in [12], where an adaptive SOC estimation strategy is presented for lead-acid batteries. A simple battery model is used with a sliding mode observer to compensate for modeling uncertainties [13]. Taking into account temperature effects, charge/discharge characteristics under different constant currents are established experimentally for a NiMH battery [14]. Then, the SOC is derived from the experimental data. In [15], an optimization

Manuscript received March 11, 2014; revised May 4, 2014 and June 6, 2014; accepted June 28, 2014. Date of publication July 22, 2014; date of current version February 6, 2015.

H. Chaoui is with the Center for Manufacturing Research, Department of Electrical and Computer Engineering, Tennessee Technological University, Cookeville, TN 38505 USA (e-mail: hchaoui@tntech.edu).

N. Golbon is with Bombardier Transportation, Kingston, ON K7K 2H6, Canada (e-mail: navidgolbon@gmail.com).

I. Hmouz and R. Souissi are with TDE Techno Design, Dollard-des-Ormeaux, QC H9B 2J5, Canada (e-mail: imad@tdetechnodesign.com; rsouissi@tdetechnodesign.com).

S. Tahar is with the Department of Electrical and Computer Engineering, Concordia University, Montreal, QC H3G 1M8, Canada (e-mail: tahar@ece.concordia.ca).

Color versions of one or more of the figures in this paper are available online at http://ieeexplore.ieee.org.

Digital Object Identifier 10.1109/TIE.2014.2341576

procedure uses measured current/voltage profiles to estimate online parameters of the battery model. This way, the model is able to capture the relevant battery dynamics and predict the SOC based on voltage estimation.

On another aspect, neural networks and fuzzy logic have been credited in various applications as powerful tools for systems subjected to structured and unstructured uncertainties [16], [17]. Several neural network models have been applied for the SOC and SOH estimation problem, which have led to a satisfactory performance [18], [19]. However, despite the success witnessed by neural networks, they remain incapable of incorporating any humanlike expertise already acquired about the dynamics of the system in hand, which is considered one of the main weaknesses of such soft-computing methodologies. In [20], a fuzzy neural network (FNN) has been proposed to overcome this weakness. These techniques are among the intelligent management systems that can monitor the SOC and gradually reduce the load to prevent continuous operation at a low SOC.

The contribution of this paper is to propose an adaptive SOC and SOH estimation technique for lithium-ion batteries. The adaptive strategy consists of a Lyapunov-based adaptation law for online parameter estimation. Therefore, the battery OCV and impedance are estimated since they vary with SOC and SOH, respectively. Thus, robustness to parametric uncertainties is achieved, which yields better accuracy as the battery ages compared to classical methods. On the other hand, soft-computing-based estimation techniques do not have such limitations, due to their learning and generalization capabilities. However, these tools suffer from a heavy computation, and tuning may not be trivial since they are based on heuristics. In this paper, we propose a Lyapunov stability-based estimation technique. Thus, stability is guaranteed unlike many classical and computational intelligence-based estimation strategies. Therefore, the proposed adaptive estimation technique achieves high accuracy and robustness, while reducing the computational burden associated with machine-learning-based techniques, which makes it realizable at low cost. Furthermore, the proposed method requires only battery voltage and current measurement, which reduces the number of sensors, with respect to other methods. The effectiveness of the proposed method is verified by simulation and experiments. The rest of the paper is organized as follows: Section II outlines the circuit model for lithium-ion batteries along with their dynamics. The proposed adaptive estimation technique is detailed in Section III. In Sections IV and V, simulation and experimental results are reported and discussed. We conclude with some remarks and suggestions for further studies pertaining to this problem.

II. Lithium-Ion Batteries

A. Modeling

Similar to other types of batteries, the lithium-ion battery has four primary components: an electrolyte, a separator, an anode, and a cathode. The electric circuit model of an electrochemical lithium-ion battery is depicted in Fig. 1. The internal battery's resistance is represented by R_b. The slow and fast *RC* network characteristic is modeled with resistances and capacitors R_s, C_s and R_f, C_f. On the other hand, the OCV–SOC characteristic

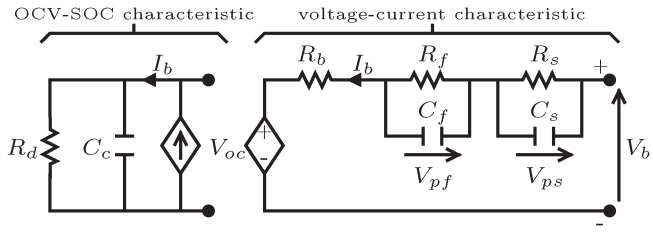

Fig. 1. Electric circuit of a lithium-ion battery.

is represented in this model by a current-controlled current source, a battery storage capacity C_c, and a self-discharge resistance R_d. A voltage-controlled voltage source is also used to bridge SOC to OCV [21].

Remark 1: It is noteworthy that, although such a model results in a drastic increase in the system's nonlinear complexity, it generally provides a more accurate representation of the system's dynamics [7], [21].

The voltage–current characteristic dynamic mathematical model can be described by the following equations [22]:

$$\dot{V}_{\rm ps} = \frac{1}{R_s C_s} V_{\rm ps} - \frac{1}{C_s} I_b \tag{1}$$

$$\dot{V}_{\rm pf} = \frac{1}{R_f C_f} V_{\rm pf} - \frac{1}{C_f} I_b \tag{2}$$

$$V_b = V_{\rm oc} + V_{\rm ps} + V_{\rm pf} + R_b I_b \tag{3}$$

where

$V_{\rm oc}$	OCV;
V_b	voltage at battery terminals;
I_b	current at battery terminals;
R_b	internal resistance;
$R_s C_s$	slow RC network;
$R_f C_f$	fast RC network;
$V_{\rm ps}$	voltage across slow RC network;
$V_{\rm pf}$	voltage across fast RC network.

B. Problem Statement

We aim to estimate the OCV $V_{\rm oc}$ and the battery's impedance since they are directly correlated to the battery's SOC and SOH. In this paper, parameters R_s, C_s, R_f, C_f, and R_b are assumed to be *a priori* unknown, and $V_{\rm ps}$, $V_{\rm pf}$ are not measurable. The system's measurable states are battery voltage V_b and current I_b. The current I_b is taken as positive in the charge mode and negative otherwise.

Assumption 1: Battery voltage V_b and current I_b along with their derivatives $\dot{V}_b$ and $\dot{I}_b$ are continuous and bounded.

Assumption 2: The OCV $V_{\rm oc}$ is a slowly time-varying signal, such that $\dot{V}_{\rm oc} \approx 0$.

Assumption 3: V_b and I_b are persistently excited.

III. Adaptive Observer

Define $e = V_b - \hat{V}_b$ as the battery voltage estimation error and the following reference model as:

$$s = e + \psi \int e = V_b - V_r \tag{4}$$

where ψ is a positive constant, and $V_r = \hat{V}_b - \psi \int e$.

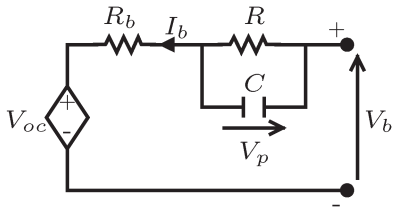

Fig. 2. Equivalent circuit model of voltage–current characteristic.

As shown experimentally in [23] and references therein, the voltage–current characteristic can be represented by the equivalent circuit model in Fig. 2, where RC is an equivalent network. Therefore, the dynamic equations can be written as

$$\dot{V}_p = \frac{1}{RC}V_p - \frac{1}{C}I_b \tag{5}$$

$$V_b = V_{\rm oc} + V_p + R_b I_b \tag{6}$$

where R and C are the equivalent resistance and capacitance, respectively.

Substituting V_p from (6) into (5) and using assumption 2 yields

$$\dot{V}_b - \frac{1}{RC}V_b - R_b\dot{I}_b + \frac{R_b}{RC}I_b + \frac{1}{C}I_b + \frac{1}{RC}V_{\rm oc} = 0.$$

Multiplying by RC yields

$$V_b = RC\dot{V}_b - R_bRC\dot{I}_b + (R + R_b)I_b + V_{\rm oc}. \tag{7}$$

This model can be represented by a regression model

$$RC\dot{V}_r - R_bRC\dot{I}_b + (R + R_b)I_b + V_{\rm oc} = \Phi^T W \tag{8}$$

where $\Phi \in \mathbb{R}^4$ is a vector of known functions (regressor), and $W \in \mathbb{R}^4$ is a vector of parameters

$$W_1 = RC$$

$$W_2 = -R_bRC$$

$$W_3 = R + R_b$$

$$W_4 = V_{\rm oc}.$$

Accurate estimation of parameter W_4 leads to a precise SOC estimation [22]. On the other hand, SOH estimation is important to determine the battery's end of life (EOL). Generally, accurate SOH estimation is obtained by capacity check using ac signal injection. However, it requires additional hardware, costly measurement, and analysis instrumentation [24]. Moreover, it requires interruption of the system's operation. Another simple way without use of additional hardware consists of monitoring the time needed for a fully charged battery to get discharged with a constant load (current). However, this also has to be performed offline, and it takes several minutes or hours to fully discharge a battery and get data regarding actual capacity. Unlike these methods, the proposed technique achieves online SOH estimation with impedance measurement while battery is in normal operation, which eliminates constraints as opposed to other methods. Studies have reported a battery impedance $R_{\rm bat}$ increase as an indication of SOH decline, which is estimated by

$$R_{\rm bat} = R_b + R_f + R_s = R_b + R = W_3.$$

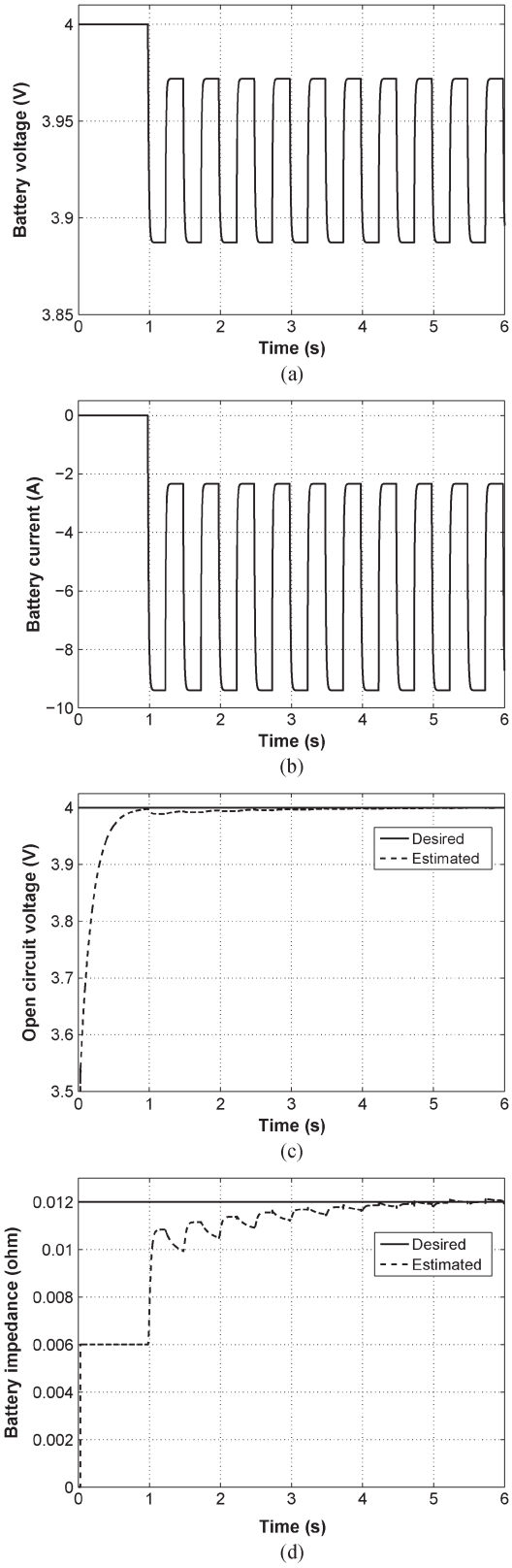

Fig. 3. System response: (a) battery's voltage V_b; (b) battery's current I_b; (c) OCV estimate $W_4 \approx V_{\rm oc}$; and (d) battery's impedance $W_3 \approx R_{\rm bat}$.

Therefore, estimating parameter W_3 leads to battery's impedance $R_{\rm bat}$ estimation. It is important to note that the proposed estimator is able to estimate $R_{\rm bat}$, regardless of the

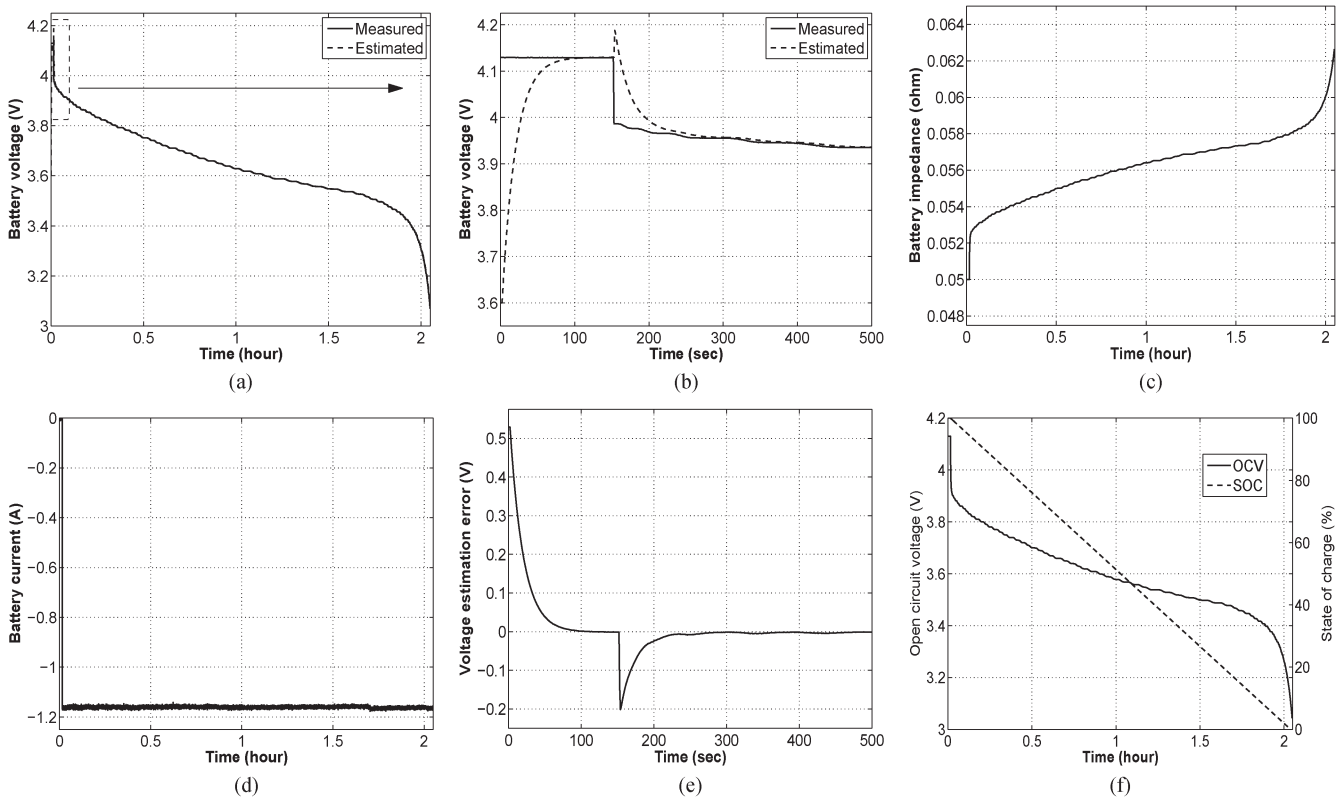

Fig. 4. Experimental results for discharge mode: (a) and (b) battery's voltage V_b; (c) battery's impedance $W_3 \approx R_{\rm bat}$; (d) battery's current I_b; (e) voltage estimation error e; and (f) OCV estimate $W_4 \approx V_{\rm oc}$ and SOC.

system's order, since individual values of $R_b, R_{f1}, R_{s1}, R_{f2}, R_{s2}, \ldots, R_{fn}, R_{sn}$ are not needed for estimation. Instead, the battery's impedance $R_{\rm bat}$ is alone sufficient for SOH estimation. On the other hand, $V_{\rm oc}$ is also independent of the order of the RC networks. Therefore, a battery's EOL impedance $R_{\rm EOL}$ is taken as 160% brand new battery's impedance $R_{\rm new}$ usually given by the manufacturer [7] (i.e., $R_{\rm EOL} = R_{\rm new} * 160\%$). Thus, SOH is expressed as

$$\text{SOH}(\%) = \frac{R_{\rm EOL} - R_{\rm bat}}{R_{\rm EOL} - R_{\rm new}} * 100\%.$$

It is noteworthy that accurate SOC estimation is guaranteed as battery ages since $R_{\rm bat}$ is among the vector of parameters W estimated by the adaptive observer. Many SOC estimation techniques are based on the knowledge of the battery's parameters, which are known to be time varying (see Figs. 3 and 4). Therefore, their performance degrades as batteries age [11]. Hence, designing an observer based on presumably accurate parameters' knowledge cannot be applied efficiently in this case. Unlike these methods, the proposed observer is adaptive and tracks parameters as they vary because of aging or other factors. On the other hand, the OCV–SOC curve is known to shift with battery aging (Fig. 5). Therefore, since battery impedance $R_{\rm bat}$ is an indication of SOH, it is used to compensate for the OCV–SOC drift due to aging. These correlation data are usually provided by manufacturers [7]. Therefore, the battery voltage estimation law is defined as follows:

$$\hat{V}_b = \Phi^T \hat{W} - K_d\, s - e \tag{9}$$

where K_d is a strictly positive constant gain.

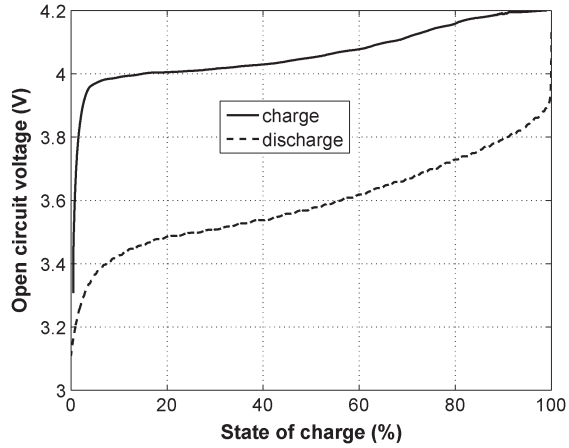

Fig. 5. Experimental results: OCV versus SOC.

Theorem 1: Consider a nonlinear system in the form of (1)–(3) with the estimation law (9). The estimation error asymptotic stability and convergence to zero are guaranteed with the following adaptation law:

$$\dot{\hat{W}} = -\Gamma\, \Phi\, s \tag{10}$$

where $\Gamma = [\gamma_1, \gamma_2, \ldots, \gamma_4]$, and γ_i is a positive constant gain.

Proof 1: Choose the following Lyapunov candidate:

$$V = \frac{1}{2}\{s^T RCs + \tilde{W}^T \Gamma^{-1} \tilde{W}\}$$

where $\tilde{W} = \hat{W} - W$. Taking the derivative of V yields

$$\dot{V} = s^T RC\dot{s} + \tilde{W}^T \Gamma^{-1} \dot{\hat{W}}. \tag{11}$$

Since parameters W are considered to be constant or slowly time-varying (assumption 2), therefore, $\dot{\tilde{W}} = \dot{\hat{W}}$. Taking the time derivative of (4) and multiplying both sides by RC yields

$$RC\dot{s} = RC\dot{V}_b - RC\dot{V}_r.$$

Substitute $RC\dot{V}_b$ from (7) as follows:

$$RC\dot{s} = -RC\dot{V}_r + R_bRC\dot{I}_b - (R + R_b)I_b - V_{\rm oc} + V_b.$$

Using the linear regression (8) yields

$$RC\dot{s} = V_b - \Phi^T W.$$

Add and subtract e, i.e.,

$$RC\dot{s} = \hat{V}_b - \Phi^T W + e.$$

Set the estimation law $\hat{V}_b$, as defined in (9), as follows:

$$RC\dot{s} = \Phi^T\tilde{W} - K_d s. \tag{12}$$

Substitute $RC\dot{s}$ from (12) into (11) as follows:

$$\dot{V} = s^T\Phi^T\tilde{W} + \tilde{W}^T\Gamma^{-1}\dot{\tilde{W}} - s^TK_ds.$$

Setting the adaptation law, as defined in (10), leads to

$$\dot{V} = -s^TK_ds < 0.$$

Since $K_d > 0$, then $\dot{V} < 0\ \forall s \neq 0$, so that $s = 0$ is a globally asymptotically stable equilibrium point. A positive Lyapunov function V, which is decreasing ($\dot{V} < 0$), must converge to a finite limit. Therefore, the system is asymptotically stable, in the sense of Lyapunov. Hence, signals s, $\tilde{W}$, and $\hat{W}$ are also bounded and converge to finite values. It implies from (4) that e and $\int e$ and, thus, $\hat{V}_b$, V_r, and $\dot{V}_r$ are bounded. It follows from (9) that V_b is bounded, which implies from (12) that $\dot{s}$ is also bounded.

Taking the derivative of $\dot{V}$ yields

$$\ddot{V} = -2s^TK_d\dot{s}.$$

Therefore, $\ddot{V}$ is also bounded.

Lemma 1: (Barbalat): If the differentiable function $V(t)$ has a finite limit as $t \to \infty$, and if $\dot{V}(t)$ is uniformly continuous, then $\dot{V}(t) \to 0$ as $t \to \infty$.

From Lemma 1, V has a finite limit as $t \to \infty$, and $\dot{V}$ is uniformly continuous. Therefore, $\lim_{t\to\infty}\dot{V} = 0$, and hence, $\lim_{t\to\infty} s = 0$. On the other hand, $\dot{e}$ is also bounded since $\dot{s}$ is bounded. From Lemma 1, $\int e$ has a finite limit as $t \to \infty$ and e is uniformly continuous shows that $\lim_{t\to\infty} e = 0$. Therefore, $\lim_{t\to\infty}\hat{V}_b = V_b$.

Remark 2: In many adaptive systems, one important aspect is the tracking error convergence. However, it gives a false impression that exponential parameter convergence is achieved. Persistent excitation condition ensures parameter convergence if the following condition:

$$\alpha_0 I_n \leq \int_{t_0}^{t_0+\beta} WW^T dt \leq \alpha_1 I_n$$

is met for all t_0, where α_0, α_1, and β are all positive, and W is the regressor vector. Note that the integral of WW^T must be positive definite and bounded over all intervals of length β. In other words, W must vary sufficiently over the interval β, so that the entire dimensional space is spanned.

TABLE I
BATTERY'S PARAMETERS

Parameter	Value	Unit
Internal resistance	$R_b = 1 \cdot 10^{-3}$	(Ω)
Resistance (slow)	$R_s = 1 \cdot 10^{-2}$	(Ω)
Capacitor (slow)	$C_s = 1 \cdot 10^{-1}$	(F)
Resistance (fast)	$R_f = 1 \cdot 10^{-3}$	(Ω)
Capacitor (fast)	$C_f = 1 \cdot 10^{-2}$	(F)

IV. Simulation Results

A. Setup

To demonstrate the performance of the proposed adaptive observer, a computer simulation is carried out on a lithium-ion battery model. The battery's model is implemented in MATLAB using a SimPowerSystems Simulink toolbox, and the sampling frequency is set to 1 KHz. Table I summarizes the battery's parameters along with their respective values. Parameters R_b, R, C, and $V_{\rm oc}$ are assumed to be *a priori* unknown and slowly time varying. The parameter estimate vector is initialized to (0, 0, $6 \cdot 10^{-2}$, 3.5), where the battery's initial impedance $R_{\rm bat}$ and OCV $V_{\rm oc}$ are set to 50% their respective desired values.

B. Results

A computer simulation is carried out to study the proposed estimator's performance. The system's response is studied, taking into account the battery's voltage V_b and current I_b, the OCV estimate $W_4 \approx V_{\rm oc}$, and the battery's impedance $W_3 \approx R_{\rm bat}$. The aforementioned nominal values are used to simulate the system's dynamics. The simulation is conducted for a time period of $t = 6$ s, where the system is left at equilibrium state for $0 \leq t < 1$ s, and the operation resumes for $1 \leq t < 6$ s. As shown in Fig. 3, a fast OCV tracking is achieved at equilibrium state ($W_4 \approx V_{\rm oc} = V_b$). It is noteworthy that, although parameter estimation needs persistent excitation in many adaptive systems, the fact that SOC can be estimated in a battery's equilibrium state makes the SOC estimator independent of this requirement. On the other hand, the battery's impedance estimation parameter stays constant since the system is not yet in operation (equilibrium state), which is consistent with regression model (8). When the system starts operating, the battery's impedance estimate converges gradually to its desired value [see Fig. 3(d)]. On the other hand, startup acts as a disturbance on the OCV estimate and causes it to deviate from its desired value. This is expected in startup since other parameter estimates did not converge yet to their respective desired values. Then, OCV starts converging gradually to its final value, as shown in Fig. 3(c).

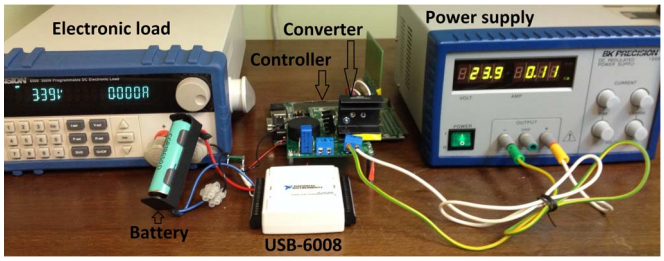

Fig. 6. Battery charger experimental setup at TDE Techno Design.

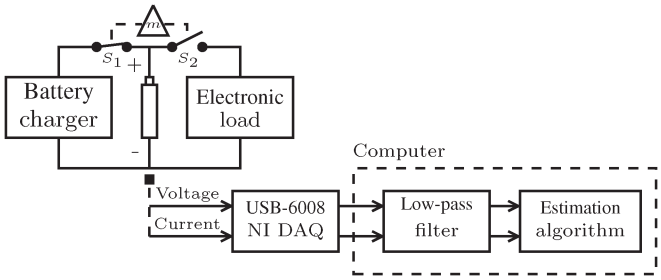

Fig. 7. Illustration of the experimental setup.

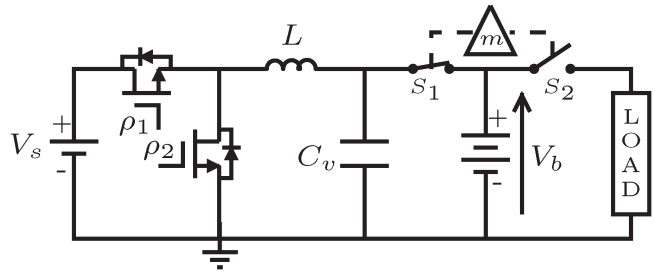

Fig. 8. Equivalent circuit of the experimental setup.

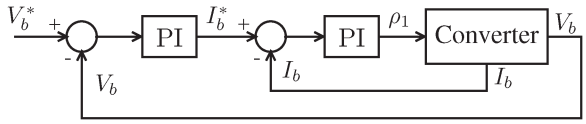

Fig. 9. Converter's control scheme.

V. Experimental Results

A. Setup

A battery charger has been designed at TDE Techno Design (see Figs. 6 and 7). It consists of a synchronous buck converter (see Fig. 8), which is controlled by conventional proportional–integral (PI) controllers, as shown in Fig. 9. A 2350-mAh 3.6-V lithium-ion battery (CGR18650D) has been used in a hardware-in-the-loop (HIL) system for validation. The SOC/SOH algorithm has been implemented using LabVIEW software, and a Universal Serial Bus (USB)-based data acquisition device (NI USB-6008) has been used as interface with the lithium-ion battery, as shown in Fig. 7. Hence, two 12-bit analog inputs are used for battery voltage and current acquisition. The control structure in Fig. 9 has been implemented in a microcontroller board (PIC24HJ256). The converter's switching frequency is set to 300 KHz, and the SOC/SOH algorithm sampling time is set to 1 s, which yields reduced computation burden once implemented in the microcontroller board. Table II summarizes the converter's parameters along with their respective values. The input voltage source is set to 24 V.

TABLE II
Converter's Parameters

Parameter	Value	Unit
Converter inductance	$L = 47$	(μH)
Converter capacitor	$C_v = 41$	(μF)

B. Results

Two experiments are carried out to validate the proposed approach. The system's response is studied taking into account the battery voltage V_b and its estimate $\hat{V}_b$, the battery voltage estimation error e, the OCV estimate $W_4 \approx V_{\rm oc}$, the battery impedance $W_3 \approx R_{\rm bat}$, and the battery current I_b. To better show convergence at startup, the battery voltage V_b and its estimate $\hat{V}_b$, along with the battery voltage estimation error e, are also shown for the first 500 s. In the first experiment, a fully charged 3.6-V lithium-ion battery is left at equilibrium state (i.e., S_1 and S_2 are both open), for the first 150 s, to show initial convergence. Then, the battery is completely discharged (i.e., S_1 open and S_2 closed), for about 2 h, at a constant rate of 1.15 A. Results are depicted in Fig. 4. The battery voltage tracking and error convergence to zero for both equilibrium and discharging states is shown in Fig. 4(b) and (e). The advantage behind the use of the adaptive observer is clearly shown by very good tracking performance and negligible amplitude, where the voltage error is kept in, i.e., 0.1%, within sensors' resolution. As the battery discharges, OCV decreases [see Fig. 4(f)] and battery impedance increases [see Fig. 4(c)]. It is important to note that battery impedance and OCV vary with the battery SOC. The relationship between the OCV and the SOC is usually given by the manufacturer. However, since these data are not available for the battery in hand, the battery's SOC is obtained through current integration to show its correlation with OCV. It is noteworthy that, although this method is known to drift due to current sensor gain/offset errors if no reset is used after a period of time, duration of experiments is not sufficient to introduce a significant error. Furthermore, the current sensor used for experiments is calibrated, and its offset is removed in the software before integration occurs. Therefore, the OCV/SOC correlation, which is also called the OCV–SOC curve, is illustrated in Fig. 5. When this curve is provided by a manufacturer, instead of experimental measurements, mapping is often performed using a curve-fitting method or a lookup table.

In the next experiment, a 3.6-V lithium-ion battery, whose initial SOC is around 5%, is subjected to a charge process (i.e., S_1 closed and S_2 open) for around 3 h. Before charging the battery, the system is left at equilibrium state (i.e., S_1 and S_2 are both open), for the first 2 min, to validate convergence in this case. Results are depicted in Fig. 10. As shown in Fig. 10(b) and (e), the adaptive observer tracks the battery voltage V_b, and the voltage estimation error decreases gradually to zero for both equilibrium and charge states. Faster convergence can

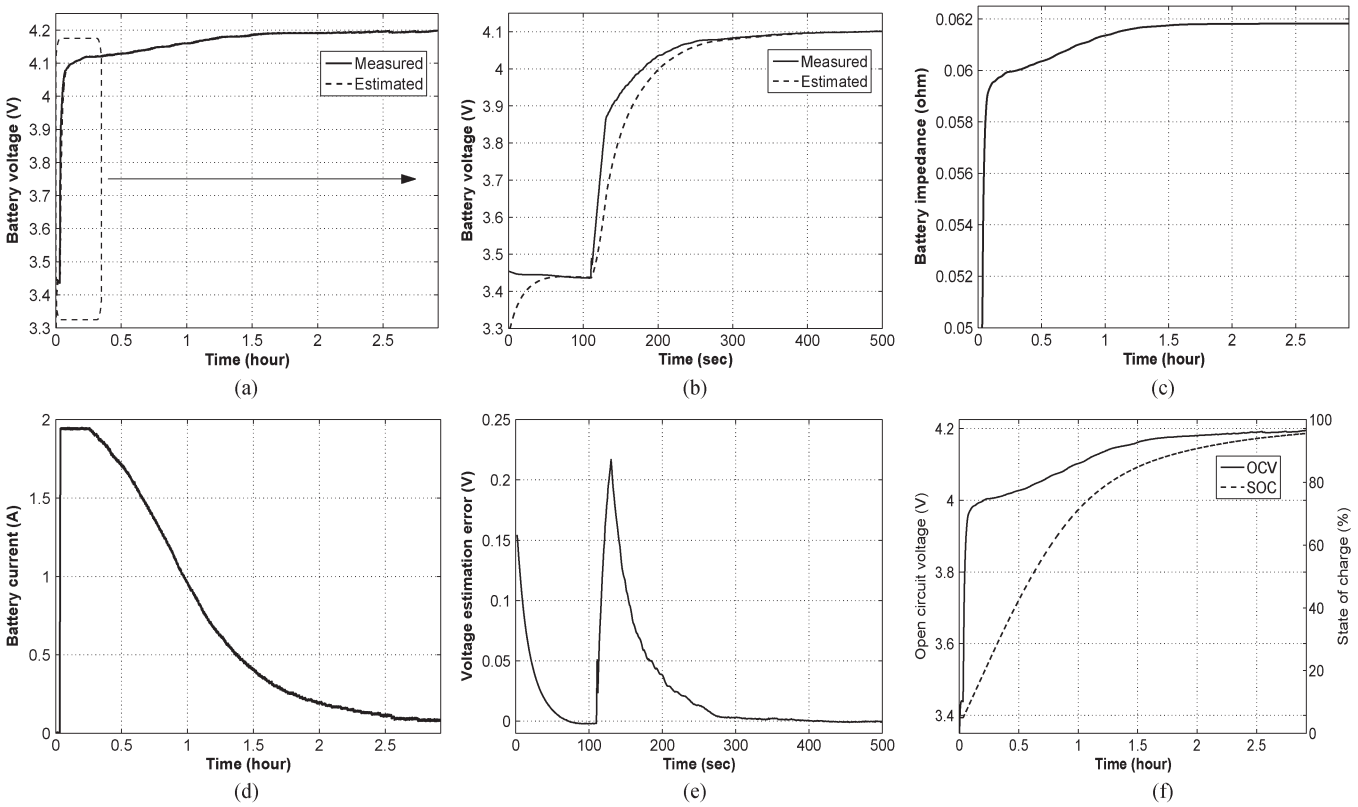

Fig. 10. Experimental results for charge mode: (a) and (b) battery's voltage V_b; (c) battery's impedance $W_3 \approx R_{\text{bat}}$; (d) battery's current I_b; (e) voltage estimation error e; and (f) OCV estimate $W_4 \approx V_{\text{oc}}$ and SOC.

be achieved by increasing adaptation parameter γ_i in (10), at the expense of more noise in the estimates. However, accuracy at steady state will be affected by noise as in any adaptive system. Therefore, there is a tradeoff between fast convergence at startup and accuracy (noise rejection). Since SOC is slowly time varying, accuracy at steady state should be given more importance. On the other hand, battery impedance convergence is also achieved. As the battery charges, current decreases continuously to zero, and OCV increases progressively since it is directly correlated with battery SOC, as shown in Fig. 10(f). It is noteworthy that the final SOC shows around 98%, which is very accurate and matches the small charge current drawn at the end of the charge process. Unlike other methods, where temperature effect is embedded in the identification model [25], this paper presents a postcompensation technique, which yields complexity reduction. Similar to aging, temperature variation introduces a drift in the OCV–SOC curve. Therefore, using temperature change $\Delta T = T_{\text{actual}} - 25\ ^\circ\text{C}$, compensation is carried out as $V_{\text{oc}}^{\text{corrected}} = V_{\text{oc}}^{25\,^\circ\text{C}} - \eta \Delta T$, where $V_{\text{oc}}^{25\,^\circ\text{C}}$ is the OCV at 25 °C (77 °F) and η is the compensation coefficient, which are both usually given by manufacturers. In addition, further experiments with a combination of various temperature and SOC/SOH conditions might be conducted to accurately determine the postcompensation coefficients. Since this paper is not about charger design's methods, the converter's efficiency and performance are briefly discussed. The charger has been designed as a "Universal Charger" with a voltage and current range from 1.2 V to 17.6 V and 200 mA to 12 A, respectively. Therefore, the converter's efficiency is revealed in Fig. 11 for different voltages and currents. As it is expected, efficiency

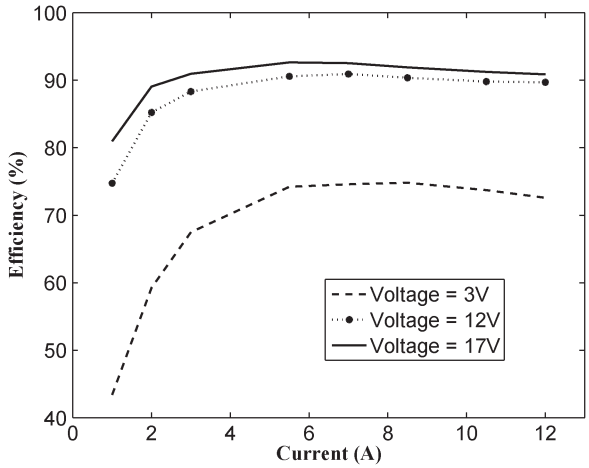

Fig. 11. Converter's efficiency.

increases with the load's power (i.e., voltage and current) to reach its maximum of 92%. It is worth mentioning that this has been achieved with hard switching. Switching losses can be significantly reduced with soft switching, which improves efficiency. However, this technique requires more complex control circuits. On the other hand, a minimum voltage ripple is expected to minimize fluctuations' impact on batteries. Therefore, the converter's voltage ripple is studied, and results are depicted in Fig. 12 for low- and high-power conditions (i.e., 3 V, 1 A and 17 V, 12 A). Voltage ripple is about 1% of the load voltage in low power, while it is decreased to around 0.5% for high power, which is acceptable for a discrete synchronous buck converter [26].

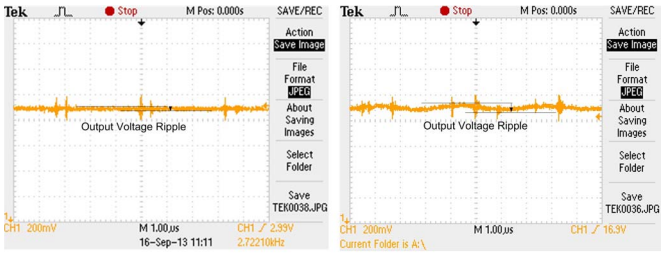

(a) (b)

Fig. 12. Converter's voltage ripple: (a) low power and (b) high power.

VI. Conclusion

In this paper, an adaptive SOC and SOH estimator has been introduced for lithium-ion batteries. The proposed strategy makes use of the capabilities of adaptive control theory to achieve robustness for online parameters estimation. The estimation technique shows that the SOC and SOH can be determined with high accuracy based on only the measurements of the battery voltage and current. Moreover, Lyapunov-based stability analysis guarantees the convergence and stability of the proposed strategy. It is easier to be implemented as opposed to other estimation approaches with similar performance, such as intelligent-based BMS. Simulation and experimental results highlight the performance of the proposed estimator in determining the SOC and SOH with high accuracy. Startup, discharge, and charge operations with constant and varying currents demonstrate the effectiveness of the adaptive estimation technique in dealing with these burdensome situations.

References

[1] M.-Y. Kim, C.-H. Kim, J.-H. Kim, and G.-W. Moon, "A chain structure of switched capacitor for improved cell balancing speed of lithium-ion batteries," *IEEE Trans. Ind. Electron.*, vol. 61, no. 8, pp. 3989–3999, Aug. 2014.

[2] A. Kuperman, U. Levy, J. Goren, A. Zafransky, and A. Savernin, "Battery charger for electric vehicle traction battery switch station," *IEEE Trans. Ind. Electron.*, vol. 60, no. 12, pp. 5391–5399, Dec. 2013.

[3] A. Ranjbar, A. Banaei, A. Khoobroo, and B. Fahimi, "Online estimation of state of charge in Li-ion batteries using impulse response concept," *IEEE Trans. Smart Grid*, vol. 3, no. 1, pp. 360–367, Mar. 2012.

[4] T. Hansen and C.-J. Wang, "Support vector based battery state of charge estimator," *J. Power Sources*, vol. 141, no. 2, pp. 351–358, Mar. 2005.

[5] S. Duryea, S. Islam, and W. Lawrance, "A battery management system for stand-alone photovoltaic energy systems," *IEEE Ind. Appl. Mag.*, vol. 7, no. 3, pp. 67–72, Jun. 2001.

[6] L. Liu *et al.*, "Integrated system identification and state-of-charge estimation of battery systems," *IEEE Trans. Energy Convers.*, vol. 28, no. 1, pp. 12–23, Mar. 2013.

[7] M. Gholizadeh and F. Salmasi, "Estimation of state of charge, unknown nonlinearities, and state of health of a lithium-ion battery based on a comprehensive unobservable model," *IEEE Trans. Ind. Electron.*, vol. 61, no. 3, pp. 1335–1344, Mar. 2014.

[8] M. Shahriari and M. Farrokhi, "Online state-of-health estimation of VRLA batteries using state of charge," *IEEE Trans. Ind. Electron.*, vol. 60, no. 1, pp. 191–202, Jan. 2013.

[9] Z. Chen, Y. Fu, and C. Mi, "State of charge estimation of lithium-ion batteries in electric drive vehicles using extended Kalman filtering," *IEEE Trans. Veh. Technol.*, vol. 62, no. 3, pp. 1020–1030, Mar. 2013.

[10] H. He, R. Xiong, X. Zhang, F. Sun, and J. Fan, "State-of-charge estimation of the lithium-ion battery using an adaptive extended Kalman filter based on an improved Thevenin model," *IEEE Trans. Veh. Technol.*, vol. 60, no. 4, pp. 1461–1469, May 2011.

[11] H. Chaoui and P. Sicard, "Accurate state of charge (SOC) estimation for batteries using a reduced-order observer," in *Proc. IEEE Int. Conf. Ind. Technol. & Southeastern Symp. Syst. Theory*, 2011, pp. 39–43.

[12] H. Chaoui, P. Sicard, and H. Ndjana, "Adaptive state of charge (SOC) estimation for batteries with parametric uncertainties," in *Proc. IEEE/ASME Adv. Intell. Mechatron. Int. Conf.*, 2010, pp. 703–707.

[13] I.-S. Kim, "Nonlinear state of charge estimator for hybrid electric vehicle battery," *IEEE Trans. Power Electron.*, vol. 23, no. 4, pp. 2027–2034, Jul. 2008.

[14] A. Szumanowski and Y. Chang, "Battery management system based on battery nonlinear dynamics modeling," *IEEE Trans. Veh. Technol.*, vol. 57, no. 3, pp. 1425–1432, May 2008.

[15] P. van Bree, A. Veltman, W. Hendrix, and P. van den Bosch, "Prediction of battery behavior subject to high-rate partial state of charge," *IEEE Trans. Veh. Technol.*, vol. 58, no. 2, pp. 588–595, Feb. 2009.

[16] H. Chaoui and P. Sicard, "Adaptive fuzzy logic control of permanent magnet synchronous machines with nonlinear friction," *IEEE Trans. Ind. Electron.*, vol. 59, no. 2, pp. 1123–1133, Feb. 2012.

[17] H. Chaoui, P. Sicard, J. Lee, and A. Ng, "Neural network modeling of cold-gas thrusters for a spacecraft formation flying test-bed," in *Proc. IEEE Conf. Ind. Electron. Soc.*, 2012, pp. 2619–2621.

[18] M. Charkhgard and M. Farrokhi, "State-of-charge estimation for lithium-ion batteries using neural networks and EKF," *IEEE Trans. Ind. Electron.*, vol. 57, no. 12, pp. 4178–4187, Dec. 2010.

[19] H.-T. Lin, T.-J. Liang, and S.-M. Chen, "Estimation of battery state of health using probabilistic neural network," *IEEE Trans. Ind. Informat.*, vol. 9, no. 2, pp. 679–685, May 2013.

[20] F.-J. Lin, M.-S. Huang, P.-Y. Yeh, H.-C. Tsai, and C.-H. Kuan, "DSP-based probabilistic fuzzy neural network control for Li-ion battery charger," *IEEE Trans. Power Electron.*, vol. 27, no. 8, pp. 3782–3794, Aug. 2012.

[21] M. Chen and G. A. Rincon-Mora, "Accurate electrical battery model capable of predicting runtime and I–V performance," *IEEE Trans. Energy Convers.*, vol. 21, no. 2, pp. 504–511, Jun. 2006.

[22] M. Petzl and M. Danzer, "Advancements in OCV measurement and analysis for lithium-ion batteries," *IEEE Trans. Energy Convers.*, vol. 28, no. 3, pp. 1–7, Sep. 2013.

[23] J. Kim, J. Shin, C. Chun, and B. Cho, "Stable configuration of a Li-ion series battery pack based on a screening process for improved voltage/SOC balancing," *IEEE Trans. Power Electron.*, vol. 27, no. 1, pp. 411–424, Jan. 2012.

[24] W. Huang and J. A. Qahouq, "An online battery impedance measurement method using DC-DC power converter control," *IEEE Trans. Ind. Electron.*, vol. 61, no. 11, pp. 5987–5995, Nov. 2014.

[25] H. Rahimi-Eichi, F. Baronti, and M.-Y. Chow, "Online adaptive parameter identification and state-of-charge coestimation for lithium-polymer battery cells," *IEEE Trans. Ind. Electron.*, vol. 61, no. 4, pp. 2053–2061, Apr. 2014.

[26] D. Diaz *et al.*, "The ripple cancellation technique applied to a synchronous buck converter to achieve a very high bandwidth and very high efficiency envelope amplifier," *IEEE Trans. Power Electron.*, vol. 29, no. 6, pp. 2892–2902, Jun. 2014.

Hicham Chaoui (S'01–M'12–SM'13) received the B.Sc. degree in electrical engineering from the Institut supérieur du Génie Appliqué (IGA), Casablanca, Morocco, in 1999, the M.Sc. degree in computer science and the Project Management Institute accredited graduate degree "Diplôme d'études Supérieures Spécialisées" in project management from the Université du Québec en Outaouais (UQO), Gatineau, QC, Canada, in 2004 and 2007, respectively, and the M.A.Sc. and Ph.D. degrees in electrical engineering from the Université du Québec à Trois-Rivières (UQTR), Trois-Rivières, QC, in 2002 and 2011, respectively.

His career has spanned both academia and industry in the field of intelligent control and renewable energies. Prior to his academic career, he held various engineering and management positions, such as Vice-President of Innovation and Technology Development at TDE Techno Design, Dollard-des-Ormeaux, QC. He is currently an Assistant Professor at Tennessee Technological University, Cookeville, TN, USA, and an Adjunct Professor at the UQTR. His research interests include adaptive and nonlinear control theory, intelligent control, robotics, mechatronics, electric motor drives, energy storage and management, real-time embedded systems, and FPGA implementation.

Dr. Chaoui was a recipient of the Best Thesis Award (health, natural science, and engineering) and the Governor General of Canada Gold Medal Award for his doctoral dissertation in 2012.

Navid Golbon (S'10–M'13) received the B.Sc. and M.Sc. degrees in electrical engineering from Isfahan University of Technology, Isfahan, Iran, and the Ph.D. degree in power electronics from the University of Western Ontario, London, ON, Canada, in 2012.

After completing the master's degree, he cofounded Behineh Niru Spadan, where he was an Electrical R&D Engineer. In 2004, he joined the National Iranian Gas Company, where he was a Senior Precise Instrument Engineer. He is currently a Power Simulation Engineer with the Systems Division, Bombardier Transportation, Kingston, ON. His research interests include power transmission and distribution, control of power plants, and design and control of power electronic converters.

Dr. Golbon is a Professional Engineer in the Province of Ontario, Canada. He was a recipient of a MITACS Grant in 2013 through Concordia University and TDE Techno Design, where he worked on the design and implementation of multibay and multichemistry smart battery chargers.

Imad Hmouz received the M.A.Sc. degree in mechanical engineering from Concordia University, Montreal, QC, Canada, in 1997.

He was an R&D Engineer and Product Development Engineer and managed a variety of projects in different areas, including renewable energy, medical devices, machine design, and automation. He is currently the CEO and Senior Design Engineer at TDE Techno Design, Dollard-des-Ormeaux, QC. His areas of expertise include product development and design of renewable energy systems, battery charging and battery management systems, structural and finite-element analysis, modular robotics and articulated arms, medical diagnosis devices, controlled drug admission devices, machine design, and automation. His research interests include renewable energy and efficient energy harvesting, power management, smart materials, manufacturing and characterization of composites, microelectromechanical systems, and nano systems.

Ridha Souissi received the B.Sc. and M.Sc. degrees in electrical engineering from Purdue University, West Lafayette, IN, USA, in 1985 and 1987, respectively.

He was an Instructor in robotics and industrial automation with the Institut Supérieur d'Électronique, Montreal, QC, Canada. From 1997 to 2006, he was an Electrical/Electronic Designer with Meggitt Training Systems Canada. After a brief assignment as an Electrical Engineer/Team Leader at Aveos Fleet Performance Inc. (formerly Air Canada Technical Services), he joined TDE Techno Design, Dollard-des-Ormeaux, QC, Canada, where he is currently an Electronic Design Engineer. His current research interest is in automatic control.

Mr. Souissi is a Professional Engineer in the Province of Quebec, Canada.

Sofiène Tahar (M'96–SM'07) received the Diploma degree in computer engineering from the University of Darmstadt, Darmstadt, Germany, in 1990 and the Ph.D. degree with distinction in computer science from the University of Karlsruhe, Karlsruhe, Germany, in 1994.

He is currently Professor and Senior Research Chair in Formal Verification of System-on-Chip with the Department of Electrical and Computer Engineering, Concordia University, Montreal, QC, Canada, where he is the Founder and Director of the Hardware Verification Group. He has made contributions and published papers in the areas of formal methods, system-on-chip verification, analog and mixed-signal circuit verification, optical systems verification, and reliability analysis of systems.

Dr. Tahar is a Professional Engineer in the Province of Quebec, Canada. He has been organizing and involved in program committees of various international conferences in the areas of formal methods and design automation. In 2007, he was named University Research Fellow upon receiving Concordia University's Senior Research Award.